

Optical conductivity of unconventional charge density wave systems: Role of vertex corrections

D.N. Aristov^{1,2,*} and R. Zeyher²

¹ *Institut für Theorie der Kondensierten Materie,
Universität Karlsruhe, 76128 Karlsruhe, Germany*

² *Max-Planck-Institut für Festkörperforschung, Heisenbergstraße 1, 70569 Stuttgart, Germany*
(Dated: September 18, 2018)

The optical conductivity of a d-CDW conductor is calculated for electrons on a square lattice and a nearest-neighbor charge-charge interaction using the lowest-order conserving approximation. The spectral properties of the Drude-like peak at low frequencies and the broad hump due to transitions across the gap at large frequencies are discussed, also as a function of temperature and of the second-nearest neighbor hopping term t' . We find that vertex corrections enhance the d.c. conductivity, make the Drude peak narrower and provide a smooth transition from a renormalized regime at low to the bare theory at high frequencies. It is also shown that vertex corrections enhance the temperature dependence of the restricted optical sum leading to a non-negligible violation of the sum rule in the d-CDW state.

PACS numbers: 71.45.Lr, 78.20.Bh, 74.72.-h

I. INTRODUCTION

The interaction between electrons may give rise to three different types of order parameters describing superconductivity, magnetism or a modulation of the charge density. As an example let us consider the Heisenberg interaction,

$$\mathcal{H}_H = \frac{J}{2} \sum_{\substack{\langle ij \rangle \\ \alpha\beta\gamma\delta}} c_{i\alpha}^\dagger \vec{\sigma}_{\alpha\beta} c_{i\beta} c_{j\gamma}^\dagger \vec{\sigma}_{\gamma\delta} c_{j\delta}. \quad (1)$$

The sum in Eq.(1) runs over nearest neighbor sites i and j , $\vec{\sigma}$ is the vector of Pauli matrices, and $c_{i\alpha}^\dagger, c_{i\alpha}$ are creation and annihilation operators for electrons at site i with spin projection α . In a mean-field treatment the expectation value of the two creation (or annihilation) operators, i.e., the order parameter, may be non-zero which leads to singlet superconductivity with extended s-wave or d-wave symmetry or triplet superconductivity with p-wave symmetry. If the average of two operators from the same site is non-zero we have a modulation of finite local spin moments describing a magnetic state. If the expectation value of two operators with the same spin projection is non-zero we deal with a charge-density wave (CDW) with an internal symmetry, because the two operators in the order parameter belong to different sites. This case will be considered in the following. For a square lattice with 4 nearest neighbors there are four different local order parameters associated with each of the four bonds which are in general complex valued but also subject to the condition that the resulting mean-field Hamiltonian must be Hermitian. The imaginary parts correspond to circulating currents expressing the breaking of time reversal symmetry.¹ The order parameters of a CDW may be classified by the point group symmetry and have in our case extended s-wave, d-wave or p-wave symmetries. Moreover, they show a modulation throughout the crystal with a wave vector \mathbf{Q} corresponding to

the total momentum of electron-hole pairs. CDW systems with an internal structure are called unconventional charge-density waves² to distinguish them from conventional ones where the electron and hole sit at the same site and do not exhibit any internal structure.

Unconventional charge-density wave systems have been invoked to explain experimental features in organic conductors,^{2,3} 2D transition metal dichalcogenides⁴ and high- T_c superconductors.^{5,6,7,8,9,10} In particular, it has been shown that a charge density wave with d-wave symmetry (d-CDW or, shortly, DDW) competes with d-wave superconductivity in the $t - J$ model in the large- N limit where N is the number of spin projections.⁶ The phase diagram of this model has a quantum critical point (QCP) separating at $T = 0$ the normal phase at large doping from a d-CDW state at lower doping if superconductivity is disregarded. Allowing also for superconductivity the QCP separates a pure superconducting state from a ground state where superconductivity and a d-CDW coexist. Due to the presence of the d-CDW the transition temperature for superconductivity exhibits a maximum, to be identified with optimal doping, and then decreases strongly in the underdoped regime. The d-CDW state exists above T_c near optimal and the underdoped region which means that the pseudogap phase should be identified with the d-CDW in this model. Various observable quantities have been calculated within this picture^{1,6,8,11,12,13,14,15,16,17,18,19} and compared with experimental data but no final conclusions have been reached.

In the following we will study the optical conductivity of a d-CDW system. In contrast to other recent work^{11,12} vertex corrections will be taken into account within a conserving approximation scheme.²⁰ Otherwise a proper definition of the current already poses a problem. Within a mean-field theory the current can be defined via the continuity equation for the charge density. The explicit calculation of the time derivative of the charge density using

the mean-field Hamiltonian of a d-CDW yields the following expression for the longitudinal current in \mathbf{k} space,²¹

$$\mathbf{j}(\mathbf{q}, t) = \frac{1}{N} \sum_{\mathbf{k}\sigma} \left[(\nabla_{\mathbf{k}} \epsilon_{\mathbf{k}}) c_{\mathbf{k}-\mathbf{q}/2\sigma}^\dagger c_{\mathbf{k}+\mathbf{q}/2\sigma} - i(\nabla_{\mathbf{k}} \Delta_{\mathbf{k}}) c_{\mathbf{k}-\mathbf{q}/2\sigma}^\dagger c_{\mathbf{k}+\mathbf{Q}+\mathbf{q}/2\sigma} \right]. \quad (2)$$

$\epsilon_{\mathbf{k}}$ and $\Delta_{\mathbf{k}}$ are one-particle energies and the d-wave order parameter, respectively. The first term in Eq.(2) is the standard expression for the current, the second one is unconventional and due to the momentum dependence of the order parameter. The use of the current definition Eq.(2) in calculating the optical conductivity guarantees that the continuity equation is satisfied²¹ but it is not a priori clear whether it is at finite frequencies more correct than the usual procedure based only on the first term in Eq.(2). In particular, one can argue that the exact interaction term in the Hamiltonian should be used in defining the current. One would then obtain only the first term in Eq.(2) because the interaction, for instance, a Heisenberg term, commutes with the density operator. Below we will show that a correct treatment defines the current only via the first term in Eq.(2) but takes vertex corrections (VC) into account. In this way the effective current at low-frequency is of the form of Eq.(2) and satisfies the continuity equation whereas it resembles more a bare current at high frequencies.

The paper is organized as follows. In the second section we introduce some properties of the Hamiltonian of a d-CDW system. In section III we derive and solve the equation for the current vertex. In section IV the optical conductivity is calculated and several limiting cases such as high and low frequencies are considered as well as the weight of the Drude peak, optical transitions and the optical sum rule. Section V contains results from a numerical evaluation of the obtained expressions, and we present our conclusions there.

II. HAMILTONIAN

We consider the following Hamiltonian for electrons on a square lattice,

$$\mathcal{H} = \sum_{\mathbf{k}\sigma} \xi_{\mathbf{k}}^{(0)} c_{\mathbf{k}\sigma}^\dagger c_{\mathbf{k}\sigma} + \frac{1}{2} \sum_{\substack{\mathbf{k}\mathbf{k}'\mathbf{k}'' \\ \sigma\sigma'}} J(\mathbf{k}-\mathbf{k}') c_{\mathbf{k}\sigma}^\dagger c_{\mathbf{k}'\sigma'} c_{\mathbf{k}''\sigma'}^\dagger c_{\mathbf{k}-\mathbf{k}'+\mathbf{k}''\sigma}. \quad (3)$$

$c_{\mathbf{k}\sigma}^\dagger$ and $c_{\mathbf{k}\sigma}$ are creation and annihilation operators for electrons with momentum \mathbf{k} and spin projection σ , respectively. $\xi_{\mathbf{k}}^{(0)}$ is equal to $\epsilon_{\mathbf{k}} - \mu$, where $\epsilon_{\mathbf{k}}$ are the bare one-particle energies and μ the chemical potential. $\epsilon_{\mathbf{k}}$ is given by $\epsilon_{\mathbf{k}} = -2t(\cos(k_x) + \cos(k_y)) + 4t'\cos(k_x)\cos(k_y)$, where t and t' denote hopping amplitudes between nearest and next-nearest neighbors, respectively. The second

term in \mathcal{H} is a Heisenberg interaction between nearest neighbors with $J(\mathbf{k}) = 2J(\cos(k_x) + \cos(k_y))$, measuring lengths in units of the lattice constant. From now on we also will measure energy in units of $2J$ which will simplify subsequent equations considerably.

Extending the spin projections from two to N the ground state of the above Hamiltonian is a charge-density wave with d-wave symmetry for some doping regime away from half-filling and large N . The corresponding wave vector is approximately $\mathbf{Q} = (\pi, \pi)$. The DDW order parameter is given by

$$\Delta_{\mathbf{k}} = \Delta \gamma_d(\mathbf{k}) = -2i\gamma_d(\mathbf{k}) \sum_{\sigma'} \int d\mathbf{k}' \gamma_d(\mathbf{k}') \langle c_{\mathbf{k}'+\mathbf{Q}\sigma'}^\dagger c_{\mathbf{k}'\sigma'} \rangle, \quad (4)$$

with $\gamma_d(\mathbf{k}) = (\cos(k_x) - \cos(k_y))/2$. Here and below our measure of integration is

$$d\mathbf{k} = dk_x dk_y / (2\pi)^2. \quad (5)$$

In the following we assume that the parameters are such that this DDW state is realized and that only the charge channel is relevant in accordance with the large N limit. It is convenient to introduce the spinors $\Psi_{\mathbf{k}\sigma}^\dagger = (c_{\mathbf{k}\sigma}^\dagger, c_{\mathbf{k}+\mathbf{Q}\sigma}^\dagger)$. The mean-field part of the Hamiltonian can then be written as

$$\mathcal{H}_{MF} = \sum_{\mathbf{k}, \sigma}' \Psi_{\mathbf{k}\sigma}^\dagger \widehat{H}_{\mathbf{k}} \Psi_{\mathbf{k}\sigma}, \quad (6)$$

with

$$\widehat{H}_{\mathbf{k}} = \begin{pmatrix} \xi_{\mathbf{k}} & i\Delta_{\mathbf{k}} \\ -i\Delta_{\mathbf{k}} & \xi_{\mathbf{k}+\mathbf{Q}} \end{pmatrix}. \quad (7)$$

The prime at the summation sign means that the sum extends only over the magnetic zone which is 1/2 of the original Brillouin zone. The mean-field contribution of the interaction term in Eq.(3) contains a diagonal part, which renormalizes $\xi_{\mathbf{k}}^{(0)}$ and yields $\xi_{\mathbf{k}}$, and a non-diagonal part, described by $\Delta_{\mathbf{k}}$. For the following it is convenient to introduce the abbreviations

$$\xi_{\pm} = (\xi_{\mathbf{k}} \pm \xi_{\mathbf{k}+\mathbf{Q}})/2, \quad (8)$$

and

$$E_{\mathbf{k}} = [\xi_{-}^2 + \Delta_{\mathbf{k}}^2]^{1/2}. \quad (9)$$

$\widehat{H}_{\mathbf{k}}$ can be diagonalized by the unitary transformation U ,

$$U = \exp(i\sigma^1 \theta_{\mathbf{k}}/2), \quad (10)$$

where $\theta_{\mathbf{k}}$ is uniquely defined by the equations

$$\cos \theta_{\mathbf{k}} = \xi_{-}/E_{\mathbf{k}}, \quad \sin \theta_{\mathbf{k}} = \Delta_{\mathbf{k}}/E_{\mathbf{k}}. \quad (11)$$

σ^i denote Pauli matrices. We have $U\widehat{H}U^\dagger = \text{diag}(\varepsilon_1, \varepsilon_2) \equiv \widehat{h}$ and the new quasiparticle energies are

$$\varepsilon_{1,2} = \xi_{\pm} \pm E_{\mathbf{k}}. \quad (12)$$

In the following we will deal with non-magnetic states which means that we may drop the spin label σ and account for sums over spin by simply inserting a factor 2. The fermionic Green's function matrix is given by

$$\widehat{G}_{\mathbf{k}}(i\omega_n) = (i\omega_n - \widehat{H})^{-1}, \quad (13)$$

where ω_n denotes the (fermionic) Matsubara frequencies $(2n+1)\pi T$. $\widehat{G}_{\mathbf{k}}$ is diagonalized by the same matrix U , so that $\widehat{G} = U^\dagger \widehat{g} U$ with $\widehat{g} = (i\omega_n - \widehat{h})^{-1}$.

III. VERTEX EQUATION

The integral equation for the current vertex is depicted graphically in Fig. 1 where the two solid lines with arrows stand for the Green's function matrix $\widehat{G}_{\mathbf{k}}(i\omega_n)$. Analytically, the integral equation reads,

$$\begin{aligned} \widehat{\Gamma}^\alpha(\mathbf{q}, i\omega_n) &= \widehat{\gamma}^\alpha(\mathbf{q}) + T \sum_{x_l} \int d\mathbf{k} J(\mathbf{k} - \mathbf{q}) \\ &\times \widehat{G}_{\mathbf{k}}(ix_l) \widehat{\Gamma}^\alpha(\mathbf{k}, i\omega_n) \widehat{G}_{\mathbf{k}}(ix_l + i\omega_n), \end{aligned} \quad (14)$$

where the current vertex $\widehat{\Gamma}^\alpha(\mathbf{q}, i\omega_n)$ is a 2x2 matrix with the elements $\Gamma_{ij}^\alpha(\mathbf{q}, i\omega_n)$. The bare current vertex $\widehat{\gamma}^\alpha(\mathbf{q})$

is diagonal and given by $\widehat{\gamma}^\alpha(\mathbf{q}) = \text{diag}(\partial_\alpha \xi_{\mathbf{q}}^{(0)}, \partial_\alpha \xi_{\mathbf{q}+\mathbf{Q}}^{(0)})$. The integration over \mathbf{k} runs over the chemical Brillouin

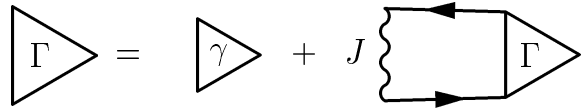


FIG. 1: Diagrammatic representation of the integral equation for the current vertex

zone, while \mathbf{q} lies within the magnetic Brillouin zone. By choosing this convention we take into account all allowed scattering processes. Eq.(14) can also be obtained by rewriting the interaction term in Nambu notation, using the diagrammatic rules and then extending the integration over \mathbf{k} throughout the chemical and not only the magnetic Brillouin zone. In Eq.(14) $i\omega_n = 2\pi i n T$ is the (bosonic) external frequency and the external momentum has been put to zero. We neglected retardation effects on the interaction amplitude $J(\mathbf{k})$ which implies that $\widehat{\Gamma}^\alpha$ depends only on one frequency variable.

Performing an analytical continuation Eq.(14) becomes,

$$\begin{aligned} \widehat{\Gamma}^\alpha(\mathbf{q}, \omega) &= \widehat{\gamma}^\alpha(\mathbf{q}) - \int \frac{dx}{2\pi i} d\mathbf{k} J(\mathbf{k} - \mathbf{q}) \left[n_F(x) \left(\widehat{G}_{\mathbf{k}}^A(x) \widehat{\Gamma}^\alpha(\mathbf{k}, \omega) \widehat{G}_{\mathbf{k}}^A(x + \omega) \right. \right. \\ &\quad \left. \left. - \widehat{G}_{\mathbf{k}}^R(x - \omega) \widehat{\Gamma}^\alpha(\mathbf{k}, \omega) \widehat{G}_{\mathbf{k}}^R(x) \right) + (n_F(x + \omega) - n_F(x)) \widehat{G}_{\mathbf{k}}^A(x) \widehat{\Gamma}^\alpha(\mathbf{k}, \omega) \widehat{G}_{\mathbf{k}}^R(x + \omega) \right]. \end{aligned} \quad (15)$$

$\widehat{G}_{\mathbf{k}}^A$ and $\widehat{G}_{\mathbf{k}}^R$ are the advanced and retarded Green's function matrices, respectively, and n_F the Fermi function. First we consider the static case, $\omega = 0$, where the last term vanishes. Inserting $\nabla_{\mathbf{k}}^\alpha \widehat{H}_{\mathbf{k}}$ for the vertex we obtain for the integral on the right-hand side of Eq.(15),

$$\begin{aligned} &\int \frac{dx}{2\pi i} d\mathbf{k} J(\mathbf{k} - \mathbf{q}) n_F(x) \left(\widehat{G}_{\mathbf{k}}^A(x) \nabla_{\mathbf{k}}^\alpha \widehat{H}_{\mathbf{k}} \widehat{G}_{\mathbf{k}}^A(x) - \widehat{G}_{\mathbf{k}}^R(x) \nabla_{\mathbf{k}}^\alpha \widehat{H}_{\mathbf{k}} \widehat{G}_{\mathbf{k}}^R(x) \right) \\ &= \int \frac{dx}{2\pi i} d\mathbf{k} J(\mathbf{k} - \mathbf{q}) n_F(x) \nabla_{\mathbf{k}}^\alpha \left(\widehat{G}_{\mathbf{k}}^A(x) - \widehat{G}_{\mathbf{k}}^R(x) \right) = \nabla_{\mathbf{q}}^\alpha \int dx d\mathbf{k} J(\mathbf{k} - \mathbf{q}) n_F(x) \widehat{G}_{\mathbf{k}}''(x) = -\nabla_{\mathbf{q}}^\alpha \widehat{\Sigma}_{\mathbf{q}}, \end{aligned} \quad (16)$$

where $2\pi i \widehat{G}_{\mathbf{k}}''(x) \equiv \widehat{G}_{\mathbf{k}}^A(x) - \widehat{G}_{\mathbf{k}}^R(x)$. Noting that the mean-field Hamiltonian is $\nabla_{\mathbf{q}}^\alpha \widehat{H}_{\mathbf{q}} = \widehat{\gamma}^\alpha(\mathbf{q}) + \nabla_{\mathbf{q}}^\alpha \widehat{\Sigma}_{\mathbf{q}}$, we observe that (15) has the solution²¹

$$\widehat{\Gamma}^\alpha(\mathbf{q}, 0) = \nabla_{\mathbf{q}}^\alpha \widehat{H}_{\mathbf{q}}. \quad (18)$$

Eq.(18) is a Ward identity relating the vertex and the self-energy in the low-frequency limit. It is a consequence of the continuity equation for charge and current densities. Since the self-energy matrix is always non-zero in the DDW state it means that the current vertex is always renormalized and never equal to the bare one. Only then

the continuity equation can be fulfilled at low frequencies. This directly shows the importance of VC in the DDW state. However, there may be special cases of interactions where VC vanish. Such a case has recently been discussed¹² where J was assumed to have the separable form $J(\mathbf{k}, \mathbf{q}) \sim f(\mathbf{q})f(\mathbf{k})$, with an even function $f(\mathbf{q}) = f(-\mathbf{q})$. For this choice of interaction the integrand in (15) is odd in \mathbf{k} , hence the integral vanishes and VC are absent.

We proceed now to solve the vertex equation Eq.(14) in the general case. The second term on the right-hand

side of (14) becomes after an analytic continuation,

$$\int d\mathbf{k} J(\mathbf{q} - \mathbf{k}) \int dx_1 dx_2 \frac{n_F(x_1) - n_F(x_2)}{\omega - x_1 + x_2 + i0} \times \widehat{G}_{\mathbf{k}}''(x_1) \widehat{\Gamma}^\alpha(\mathbf{k}, \omega) \widehat{G}_{\mathbf{k}}''(x_2). \quad (19)$$

Using the unitary transformation U of Eq.(10) the Green's function matrix can be written as $\widehat{G}_{\mathbf{k}} = U_{\mathbf{k}}^\dagger \widehat{g}_{\mathbf{k}} U_{\mathbf{k}}$ with a diagonal $\widehat{g}_{\mathbf{k}}$. The product of the three matrices in (19) can be represented as $U^\dagger \widehat{g}''(x_1) \widehat{\Gamma}^\alpha \widehat{g}''(x_2) U$ with $\widehat{\Gamma}^\alpha = U \widehat{\Gamma}^\alpha U^\dagger$. Next we expand $\widehat{\Gamma}^\alpha$ in terms of Pauli matrices

$$\widehat{\Gamma}^\alpha = \sum_i \Gamma_i^\alpha \sigma_i. \quad (20)$$

The s -wave component of the current, Γ_1^α , is in general allowed by Eq.(15) but vanishes if J is a nearest-neighbor interaction. Hence we restrict ourselves to three components and write $\widehat{\Gamma}^\alpha = \Gamma_0^\alpha \sigma_0 + \Gamma_3^\alpha \sigma_3 + \Gamma_2^\alpha \sigma_2$, and similarly for the transformed vertex, $\widetilde{\Gamma}^\alpha = \Gamma_0^\alpha \sigma_0 + \widetilde{\Gamma}_3^\alpha \sigma_3 + \widetilde{\Gamma}_2^\alpha \sigma_2$. Using the explicit form for U we obtain

$$\begin{pmatrix} \widetilde{\Gamma}_3^\alpha \\ \widetilde{\Gamma}_2^\alpha \end{pmatrix} = \begin{pmatrix} \cos \theta_k & -\sin \theta_k \\ \sin \theta_k & \cos \theta_k \end{pmatrix} \begin{pmatrix} \Gamma_3^\alpha \\ \Gamma_2^\alpha \end{pmatrix} \equiv \widehat{T} \begin{pmatrix} \Gamma_3^\alpha \\ \Gamma_2^\alpha \end{pmatrix}. \quad (21)$$

The diagonal components of the expression

$$I = \int dx_1 dx_2 \frac{n_F(x_1) - n_F(x_2)}{\omega - x_1 + x_2 + i0} \widehat{g}''(x_1) \widetilde{\Gamma}^\alpha \widehat{g}''(x_2) \quad (22)$$

are regularized at $\omega \rightarrow 0$ in the presence of impurity scattering. We adopt the simplest picture of point-like scatterers, characterized by the inverse quasiparticle lifetime τ . Note that isotropic scattering from such impurities allows us to neglect VC and to include τ only in

the Green's function. The Green's functions take then the form $\widehat{g}^R(x) = \text{diag}[g_{1,\mathbf{k}}^R(x), g_{2,\mathbf{k}}^R(x)]$, where $g_{j,\mathbf{k}}^R(x) = (x - \varepsilon_{j,\mathbf{k}} + i/(2\tau))^{-1}$. A standard calculation gives for the 11 element of I in the limit of small $\tau^{-1} \ll T$,

$$\begin{aligned} & (\Gamma_0^\alpha + \widetilde{\Gamma}_3^\alpha) \int dx_1 dx_2 \frac{n_F(x_1) - n_F(x_2)}{\omega - x_1 + x_2 + i0} g_{1,\mathbf{k}}''(x_1) g_{1,\mathbf{k}}''(x_2) \\ &= \frac{-n'_F(\varepsilon_{1,\mathbf{k}})}{1 - i\omega\tau} (\Gamma_0^\alpha + \widetilde{\Gamma}_3^\alpha), \end{aligned} \quad (23)$$

where $n'_F(x)$ is the derivative of the Fermi function. The non-diagonal components of I are given by the expression

$$\sigma_2 \frac{\widetilde{\Gamma}_2^\alpha}{2} \left[\frac{n_F(\varepsilon_{1,\mathbf{k}}) - n_F(\varepsilon_{2,\mathbf{k}})}{\omega + i/\tau - \varepsilon_{1,\mathbf{k}} + \varepsilon_{2,\mathbf{k}}} + (1 \leftrightarrow 2) \right].$$

Introducing shorthand notations,

$$z \equiv (1 - i\omega\tau)^{-1}, \quad (24)$$

$$\rho_j \equiv -n'_F(\varepsilon_{j,\mathbf{k}}), \quad (25)$$

$$\rho_\pm \equiv (\rho_1 \pm \rho_2)/2, \quad (26)$$

$$K = \frac{n_F(\varepsilon_{1,\mathbf{k}}) - n_F(\varepsilon_{2,\mathbf{k}})}{(\varepsilon_{2,\mathbf{k}} - \varepsilon_{1,\mathbf{k}})^2 - (\omega + i/\tau)^2} (\varepsilon_{2,\mathbf{k}} - \varepsilon_{1,\mathbf{k}}), \quad (27)$$

we have

$$I = \sigma_0 z (\rho_+ \Gamma_0^\alpha + \rho_- \widetilde{\Gamma}_3^\alpha) + \sigma_3 z (\rho_- \Gamma_0^\alpha + \rho_+ \widetilde{\Gamma}_3^\alpha) + \sigma_2 K \widetilde{\Gamma}_2^\alpha. \quad (28)$$

The next step in the evaluation of (19) is to carry out the rotation $U^\dagger I U$. Suppressing the dependence on the external frequency in the notation we obtain from Eq.(14), the following system of coupled equations,

$$\Gamma_0^\alpha(\mathbf{q}) = \gamma_0^\alpha(\mathbf{q}) + z \int d\mathbf{k} J(\mathbf{q} - \mathbf{k}) (\rho_+ \Gamma_0^\alpha + \rho_- \widetilde{\Gamma}_3^\alpha) \quad (29)$$

$$\begin{pmatrix} \Gamma_3^\alpha(\mathbf{q}) \\ \Gamma_2^\alpha(\mathbf{q}) \end{pmatrix} = \begin{pmatrix} \gamma_3^\alpha(\mathbf{q}) \\ 0 \end{pmatrix} + \int d\mathbf{k} J(\mathbf{q} - \mathbf{k}) \widehat{T}^\dagger \left[\begin{pmatrix} z \rho_- \Gamma_0^\alpha(\mathbf{k}) \\ 0 \end{pmatrix} + \begin{pmatrix} z \rho_+ & 0 \\ 0 & K \end{pmatrix} \widehat{T} \begin{pmatrix} \Gamma_3^\alpha(\mathbf{k}) \\ \Gamma_2^\alpha(\mathbf{k}) \end{pmatrix} \right] \quad (30)$$

A further simplification to Eqs. (29), (30) results from the nearest-neighbor form of the interaction $J(\mathbf{k})$. In this case the integral in (29) vanishes, which can be seen by considering a shift $\mathbf{q} \rightarrow \mathbf{q} + \mathbf{Q}$; upon this shift γ_0^α is unchanged and $J(\mathbf{k} - \mathbf{q}) \rightarrow -J(\mathbf{k} - \mathbf{q})$. The ‘‘symmetrical’’ component of the current is thus not renormalized and given by $\Gamma_0^\alpha(\mathbf{q}) = \gamma_0^\alpha(\mathbf{q}) = \nabla^\alpha \xi_+$.

In order to solve Eq.(30) we note that $\gamma_3^\alpha(\mathbf{q})$ transforms like a vector, i.e., according to the representation Γ_5 of the point group C_{4v} . Decomposing $J(\mathbf{k} - \mathbf{q})$ into separ-

able kernels only $\sin(k_\alpha) \sin(q_\alpha)$ can contribute because $\sin(k_\alpha)$ is the only function appearing in the decomposition which transforms according to the representation Γ_5 . Taking into account the transformation properties of \widehat{T} under C_{4v} one finds that this argument applies also to Γ_2^α . The solution of Eq.(30) has thus the form,

$$\Gamma_3^\alpha(\mathbf{q}) = \gamma_3^\alpha(\mathbf{q}) + \sin(q_\alpha) c_3^\alpha, \quad (31)$$

$$\Gamma_2^\alpha(\mathbf{q}) = \sin(q_\alpha) c_2^\alpha. \quad (32)$$

The coefficients c_3^α, c_2^α depend still on the external fre-

quency but no longer on momentum. It is convenient to introduce the notation

$$\widehat{\gamma}_0^\alpha = \begin{pmatrix} \rho_- \gamma_0^\alpha \\ 0 \end{pmatrix}, \quad \widehat{\gamma}_3 = \begin{pmatrix} \gamma_3^\alpha \\ 0 \end{pmatrix}, \quad (33)$$

$$\widehat{V} = \widehat{T}^\dagger \begin{pmatrix} z\rho_+ & 0 \\ 0 & K \end{pmatrix} \widehat{T}. \quad (34)$$

and

$$\widehat{d} = \int d\mathbf{k} \sin(k_\alpha) (z\widehat{T}^\dagger \widehat{\gamma}_0 + \widehat{V} \widehat{\gamma}_3), \quad (35)$$

$$\widehat{X} = \int d\mathbf{k} \sin^2(k_\alpha) \widehat{V}. \quad (36)$$

Using this notation and the vectors

$$\widehat{c} = \begin{pmatrix} c_3^\alpha \\ c_2^\alpha \end{pmatrix}, \quad \widehat{d} = \begin{pmatrix} d_3^\alpha \\ d_2^\alpha \end{pmatrix}, \quad (37)$$

one represents Eq. (30) in the following form

$$\widehat{c} = \widehat{d} + \widehat{X} \widehat{c}, \quad (38)$$

Using Eq.(11) more explicit expressions for the elements of \widehat{V} and for \widehat{d} can easily be obtained,

$$V_{11} = (z\rho_+ \xi_-^2 + K \Delta_{\mathbf{k}}^2) / E_{\mathbf{k}}^2, \quad (39a)$$

$$V_{12} = V_{21} = \xi_- \Delta_{\mathbf{k}} (K - z\rho_+) / E_{\mathbf{k}}^2, \quad (39b)$$

$$V_{22} = (z\rho_+ \Delta_{\mathbf{k}}^2 + K \xi_-^2) / E_{\mathbf{k}}^2, \quad (39c)$$

and

$$d_3^\alpha = \int d\mathbf{k} \sin(k_\alpha) \left[z \frac{\rho_- \gamma_0^\alpha \xi_-}{E_{\mathbf{k}}} + \gamma_3^\alpha V_{11} \right], \quad (40a)$$

$$d_2^\alpha = \int d\mathbf{k} \sin(k_\alpha) \left[-z \frac{\rho_- \gamma_0^\alpha \Delta_{\mathbf{k}}}{E_{\mathbf{k}}} + \gamma_3^\alpha V_{21} \right]. \quad (40b)$$

IV. OPTICAL CONDUCTIVITY

The frequency-dependent conductivity is given by one current loop with one renormalized and one bare vertex. Analytically it is given by the following expression,

$$\sigma(\omega) = \omega^{-1} Im \int d\mathbf{k} \int dx_1 dx_2 \frac{n_F(x_1) - n_F(x_2)}{\omega - x_1 + x_2 + i0} Tr[\widehat{\gamma}^\alpha(\mathbf{k}) \widehat{G}_{\mathbf{k}}''(x_1) \widehat{\Gamma}^\alpha(\mathbf{k}, \omega) \widehat{G}_{\mathbf{k}}''(x_2)] \quad (41)$$

Eq. (41) allows the same analysis as was done above for the vertex, (cf. (19)). The integration over $x_{1,2}$ yields

$$\sigma(\omega) = \omega^{-1} Im \int d\mathbf{k} Tr[\widehat{\gamma}^\alpha(\mathbf{k}) U^\dagger I U], \quad (42)$$

with I given by (28). The integration is over the magnetic Brillouin zone. The trace in the last formula is represented as

$$\frac{1}{2} Tr[\dots] = z\gamma_0^\alpha(\mathbf{k})(\rho_+ \gamma_0^\alpha + \rho_- \widetilde{\Gamma}_3^\alpha) + (\gamma_3^\alpha(\mathbf{k}), 0) \widehat{T}^\dagger \left[\begin{pmatrix} z\rho_- \gamma_0^\alpha(\mathbf{k}) \\ 0 \end{pmatrix} + \begin{pmatrix} z\rho_+ & 0 \\ 0 & K \end{pmatrix} \widehat{T} \begin{pmatrix} \Gamma_3^\alpha(\mathbf{k}) \\ \Gamma_2^\alpha(\mathbf{k}) \end{pmatrix} \right]. \quad (43)$$

Eqs.(42) and (43) can be recast in the form

$$\sigma(\omega) = Im Q / \omega, \quad (44)$$

$$Q = z(a_0 + 2a_1) + a_2 + \widehat{d}^\dagger \widehat{c}. \quad (45)$$

The numbers a_0, a_1, a_2 are given by

$$a_0 = \int d\mathbf{k} (\gamma_0^\alpha)^2 \rho_+, \quad (46a)$$

$$a_1 = \int d\mathbf{k} \widehat{\gamma}_3^\dagger \widehat{T}^\dagger \widehat{\gamma}_0 = \int d\mathbf{k} \gamma_3^\alpha \gamma_0^\alpha \rho_- \xi_- / E_{\mathbf{k}}, \quad (46b)$$

$$a_2 = \int d\mathbf{k} \widehat{\gamma}_3^\dagger \widehat{V} \widehat{\gamma}_3 = \int d\mathbf{k} (\gamma_3^\alpha)^2 V_{11}. \quad (46c)$$

The dagger at the column vectors denote the transposed vectors, i.e., row vectors. Solving Eq. (38) we obtain from

Eq. (45)

$$Q = z(a_0 + 2a_1) + a_2 + \widehat{d}^\dagger (1 - \widehat{X})^{-1} \widehat{d}. \quad (47)$$

The frequency dependence of Q is due to the functions F and K which also enter \widehat{V} and thus \widehat{d} , \widehat{X} and the vertex.

A. Conductivity at zero and at high frequencies

In the limit $\omega \rightarrow 0$, the conductivity may be determined from the relation

$$\sigma(\omega = 0) = \tau(dQ/dz)|_{z=1}. \quad (48)$$

Writing $a_2 = za_{21} + a_{22}$ and $\hat{d} = z\hat{D}_1 + \hat{D}_2$ we obtain with $A = a_0 + 2a_1 + a_{21}$,

$$\sigma(\omega = 0) = \tau(A + \hat{D}_1^\dagger \hat{c} + \hat{d}^\dagger \hat{c}')|_{z=1}, \quad (49)$$

where $\hat{c}' = (d\hat{c}/dz)$ Differentiating Eq.(38) with respect to z ,

$$(1 - \hat{X})\hat{c} = \hat{d}, \quad (50)$$

and writing $\hat{X} = z\hat{X}_1 + \hat{X}_2$ we obtain

$$(1 - \hat{X})\hat{c}' = \hat{D}_1 + \hat{X}_1\hat{c}. \quad (51)$$

Multiplying Eq.(50) from the left with \hat{c}'^\dagger and using Eq.(51) we find for the last term in Eq.(49),

$$\hat{d}^\dagger \hat{c}' = \hat{D}_1^\dagger \hat{c} + \hat{c}'^\dagger \hat{X}_1^\dagger \hat{c}. \quad (52)$$

Using the abbreviation $\hat{c}_0 \equiv \hat{c}|_{z=1}$ we have

$$\sigma(\omega = 0) = \tau(A + 2\hat{D}_1^\dagger \hat{c}_0 + \hat{c}_0^\dagger \hat{X}_1 \hat{c}_0). \quad (53)$$

The last expression is not very transparent, but one can check that it exactly corresponds to the naive symmetrization of (41) using the static mean-field vertex $\hat{\Gamma}^\alpha(\mathbf{k}, 0)$,

$$\begin{aligned} \sigma(\omega)_{naive} &= \omega^{-1} Im \int d\mathbf{k} \int dx_1 dx_2 \frac{n_F(x_1) - n_F(x_2)}{\omega - x_1 + x_2 + i0} \\ &\times Tr[\hat{\Gamma}^\alpha(\mathbf{k}, 0)\hat{G}_{\mathbf{k}}''(x_1)\hat{\Gamma}^\alpha(\mathbf{k}, 0)\hat{G}_{\mathbf{k}}''(x_2)], \end{aligned} \quad (54)$$

in the limit $\omega \rightarrow 0$. This result for a simpler case without DDW order is usually attributed to Langer.²²

Consider now the ‘‘tail’’ of the Drude peak which corresponds to $\omega\tau \gg 1$ or $|z| \ll 1$ and $K \equiv K(0)$. From Eq.(45) we obtain in linear order in z ,

$$\begin{aligned} Q &= z(A + \hat{D}_1^\dagger(1 - \hat{X}_2)^{-1}\hat{D}_2 \\ &+ \hat{D}_2^\dagger(1 - \hat{X}_2)^{-1}\hat{X}_1(1 - \hat{X}_2)^{-1}\hat{D}_2 \\ &+ \hat{D}_2^\dagger(1 - \hat{X}_2)^{-1}\hat{D}_1). \end{aligned} \quad (55)$$

Using $\hat{c}|_{z=0} = (1 - \hat{X}_2)^{-1}\hat{D}_2$ we find,

$$\sigma(\omega\tau \gg 1) \simeq \frac{1}{\omega^2\tau}(A + 2\hat{D}_1^\dagger \hat{c} + \hat{c}'^\dagger \hat{X}_1 \hat{c})|_{z=0}. \quad (56)$$

Eqs.(40a) and (40b) show that the two last terms in Eq.(56) are roughly by a factor $J\Delta_0^2/t^3$ smaller than the first three terms. Since in practice $J\Delta_0^2/t^3 \ll 1$ we may drop the last two terms in Eq.(56) and obtain approximately,

$$\sigma(\omega\tau \gg 1) \simeq \frac{A}{\omega^2\tau}. \quad (57)$$

Eq.(57) shows that the current vertex changes from its mean-field value Eq.(18) near the maximum of the Drude peak to its bare value in the tail of the Drude peak. The renormalization of the current vertex is important at low

frequencies where it contributes to satisfy the continuity equation of charge. At higher frequencies this renormalization is stripped off and the bare value of the vertex determines the behavior in the Drude tail. This observation is not surprising, because the overall prefactor τ^{-1} shows that impurity scattering contributes in the lowest order. The inclusion of the scattering process into the corresponding current loop effectively breaks the diagram into two unconnected parts with their vertices. It is easy to understand that these vertices are described by i) small but finite incoming frequency ω , ii) the full inclusion of the J term, and iii) the Green functions without damping τ^{-1} . The result of the vertex summation in this limit is given by solving (38) at $z = 0$ which leads to $\hat{\Gamma}^\alpha \simeq \hat{\gamma}^\alpha$ in leading order in Δ_0/t .

B. Weight of the Drude peak

The weight of the Drude peak is given by integration of the above σ over ω for $K(\omega) \equiv K(0)$. We define the spectral weight of the Drude peak as $W_D = \pi^{-1} \int d\omega Im Q/\omega$. The function $Q(z)$ is an analytical function of the complex variable $z = 1/(1 - i\omega\tau)$ in the circle $|z - 1/2| < 1/2$, which corresponds to analyticity in the upper semiplane of ω . Performing a Taylor expansion around $z = 0$ (a more accurate expansion around $z = 1/2$ leads to the same result), we write $Q(z) = \sum_{n \geq 0} Q_n z^n$ and obtain,

$$\begin{aligned} W_D &= \frac{1}{\pi} \int \frac{d\omega}{\omega} Im \sum_{n \geq 0} \frac{Q_n}{(1 - i\omega\tau)^n} \\ &= \sum_{n \geq 1} Q_n = Q(z = 1) - Q(z = 0). \end{aligned} \quad (58)$$

From Eq.(45) we have

$$\begin{aligned} W_D &= A + R, \\ R &= (\hat{D}_1^\dagger + \hat{D}_2^\dagger)(1 - \hat{X}_1 - \hat{X}_2)^{-1}(\hat{D}_1 + \hat{D}_2) \\ &\quad - \hat{D}_2^\dagger(1 - \hat{X}_2)^{-1}\hat{D}_2. \end{aligned} \quad (59)$$

Inserting the identity

$$\begin{aligned} (1 - \hat{X}_1 - \hat{X}_2)^{-1} &= (1 - \hat{X}_2)^{-1} \\ &\quad + (1 - \hat{X}_2)^{-1}\hat{X}_1(1 - \hat{X}_1 - \hat{X}_2)^{-1}, \end{aligned}$$

into the first term of R and using

$$(1 - \hat{X}_1 - \hat{X}_2)^{-1}\hat{d} = \hat{c}_0, \quad (61)$$

$$(1 - \hat{X}_2)^{-1}\hat{d} = \hat{c}_0 - (1 - \hat{X}_2)^{-1}\hat{X}_1\hat{c}_0, \quad (62)$$

we obtain

$$R = \hat{D}_1^\dagger \hat{c}_0 + \hat{D}_2^\dagger(1 - \hat{X}_2)^{-1}(\hat{D}_1 + \hat{X}_1\hat{c}_0). \quad (63)$$

Writing $\hat{D}_2^\dagger = \hat{d}^\dagger - \hat{D}_1^\dagger$ in the second term on the right-hand side of Eq.(63), using the transposed equation of

Eq.(62), and inserting the result into Eq.(59) one finds

$$W_D = A + 2\widehat{D}_1^\dagger \widehat{c}_0 + c_0^\dagger \widehat{X}_1 \widehat{c}_0 - (c_0^\dagger \widehat{X}_1 + \widehat{D}_1^\dagger)(1 - \widehat{X}_2)^{-1}(\widehat{D}_1 + \widehat{X}_1 \widehat{c}_0). \quad (64)$$

Without the last term in Eq.(64) W_D would be equal to the spectral weight of a simple Lorentzian of the form $\sigma_D(\omega) = \sigma(0)/(1 + \omega^2\tau^2)$ with $\sigma(0)$ given by Eq.(53). From Eq.(39) follows that $1 - X_{ij}$ is a positive definite matrix for $\Delta_0/t \ll 1$. Stability arguments suggest that this should be generally true as long as the DDW state is thermodynamically stable. It follows that the last term in Eq.(64) is negative and thus reduces the spectral weight compared to that of a Lorentzian form for $\sigma(\omega)$.

C. Optical transitions

At finite frequencies of the order of Δ_0 the Drude contribution to $\sigma(\omega)$ is small and can be neglected whereas the frequency dependence of $K(\omega)$ becomes important. Putting $z = 0$ and showing the frequency dependencies explicitly Eqs.(38) and (45) take the form,

$$\widehat{c} = \widehat{D}_2(\omega) + \widehat{X}_2(\omega)\widehat{c} \quad (65)$$

$$Q = a_{22}(\omega) + \widehat{D}_2^\dagger(\omega)\widehat{c}. \quad (66)$$

If $\widehat{X}_2, \widehat{d}_2$ and a_{22} are purely real, then $\sigma(\omega) = ImQ/\omega = 0$. This situation happens at $T = 0$, when ω lies within the optical gap of $K(\omega)$. At frequencies above the threshold value, which is twice the value of the gap at the hot spots, i.e., $\omega \gtrsim 2\Delta_{hs}$, the optical conductivity is finite. From Eqs.(65) and (66) follows that

$$Q = a_{22}(\omega) + \widehat{D}_2^\dagger(\omega)(1 - \widehat{X}_2(\omega))^{-1}\widehat{D}_2(\omega). \quad (67)$$

The second term on the right-hand side of Eq.(67) is due to VC and has been neglected in a previous work.¹¹

D. Restricted optical sum

Finally we discuss the restricted optical sum, given by the expression $W = \pi^{-1} \int_{-\infty}^{\infty} d\omega ImQ/\omega$. From the Kramers-Kronig relations we find

$$W = Q(\omega = 0) - Q(\omega = \infty). \quad (68)$$

The subtraction of the term $Q(\omega = \infty)$ reflects the fact that the Kramers-Kronig relation recovers the real part of the function up to a constant, which is $Q(\omega = \infty)$. The latter quantity is given by taking the limit $\omega \rightarrow \infty$ in Eq.(67). From the explicit expressions Eqs.(39)-(40b) one finds $Q(\omega = \infty) = 0$. Furthermore we have,

$$Q(\omega = 0) \equiv Q(z = 1) = (A + a_{22} + \widehat{d}^\dagger \widehat{c})|_{z=1}. \quad (69)$$

Performing a similar calculation as in the case of the Drude weight we find

$$W = W_D + (a_{22} + \widehat{D}_2^\dagger(1 - \widehat{X}_2)^{-1}\widehat{D}_2)|_{z=1}. \quad (70)$$

Comparing with Eq.(67) one recognizes that the sum of the second and third terms on the right-hand side of Eq.(70) represents just the spectral weight due to optical transitions as it should be.

V. NUMERICAL RESULTS AND CONCLUSIONS

Introducing the unperturbed Hamiltonian $\widehat{H}_{\mathbf{k}}^{(0)}$ by

$$\widehat{H}_{\mathbf{k}}^{(0)} = \begin{pmatrix} \xi_{\mathbf{k}}^{(0)} & 0 \\ 0 & \xi_{\mathbf{k}+\mathbf{Q}}^{(0)} \end{pmatrix}, \quad (71)$$

the self-energy $\widehat{\Sigma}_{\mathbf{k}}$ can be written as

$$\widehat{\Sigma}_{\mathbf{k}} = \widehat{H}_{\mathbf{k}} - \widehat{H}_{\mathbf{k}}^{(0)} = \begin{pmatrix} \delta\xi_{\mathbf{k}} & i\Delta_{\mathbf{k}} \\ -i\Delta_{\mathbf{k}} & \delta\xi_{\mathbf{k}+\mathbf{Q}} \end{pmatrix}. \quad (72)$$

After dropping the derivative $\nabla_{\mathbf{k}}^\alpha$, Eq.(17) represents a self-consistent matrix equation for $\widehat{\Sigma}_{\mathbf{k}}$. The resulting gap equation reads, using $2J$ as the energy unit,

$$1 = -2 \int d\mathbf{k} \gamma_d^2(\mathbf{k}) \frac{n_F(\epsilon_{1\mathbf{k}}) - n_F(\epsilon_{2\mathbf{k}})}{\epsilon_{1\mathbf{k}} - \epsilon_{2\mathbf{k}}}. \quad (73)$$

The renormalization of the diagonal part of $\widehat{\Sigma}_{\mathbf{k}}$ becomes $\delta\xi_{\mathbf{k}}^+ = 0$ and, writing $\delta\xi_{\mathbf{k}}^- = b\gamma_s(\mathbf{k})$, $\gamma_s = \frac{1}{2}(\cos(k_x) + \cos(k_y))$,

$$b = -2 \int d\mathbf{k} \gamma_s(\mathbf{k}) \xi_{\mathbf{k}}^- \frac{n_F(\epsilon_{1\mathbf{k}}) - n_F(\epsilon_{2\mathbf{k}})}{\epsilon_{1\mathbf{k}} - \epsilon_{2\mathbf{k}}}. \quad (74)$$

We have solved Eqs.(73) and(74) by iteration. For $T = 0, t = 0.25, t' = 0.075$ we find that Δ is non-zero in the interval $0.35 < n_\sigma < 0.50$, increases linearly in this interval from 0.15 to 0.19, and shows a step-like behavior at the ends of this interval. n_σ is the occupation of one site for one spin direction. b is practically constant in the above interval and equal to -0.39 . Fig.2 shows Δ and b as a function of temperature for a fixed occupancy $n_\sigma = 0.40$. b is again practically a constant whereas Δ exhibits a BCS-like temperature dependence with $T_c \sim 0.07$.

Using the above values for Δ and b Fig.3 shows the optical conductivity $\sigma(\omega)$ calculated with (solid line) and without (dashed line) VC for the parameters indicated in the figure. "Without VC" means the use of the bare vertex, i.e., to put c_2^z and c_3^z in Eqs.(31) and (32) to zero. In the presence of a finite Δ the Fermi lines are folded back into the small magnetic Brillouin zone, a gap opens near the new phase boundary in \mathbf{k} space, and the resulting Fermi lines consist of arcs around the nodal direction and small pieces near the points $X = (\pi, 0)$ and $Y = (0, \pi)$. The low-frequency Drude-like behavior of $\sigma(\omega)$ is due to electrons near the remnant Fermi lines, especially near the arcs around the diagonal directions.¹⁹ The hump at frequencies above 0.2 is caused by vertical transitions between the two back-folded bands in the

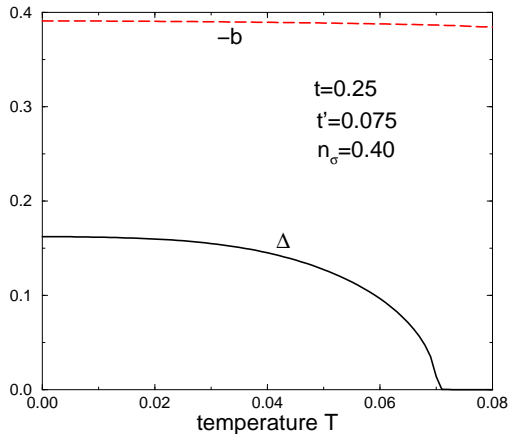


FIG. 2: Spectral gap Δ_0 and the parameter b as a function of temperature T , using $2J$ as the energy unit.

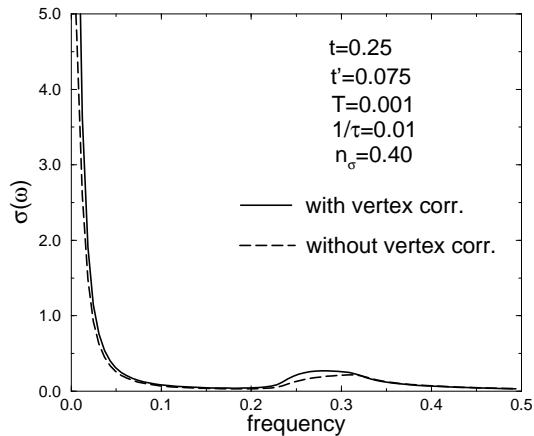


FIG. 3: Optical conductivity $\sigma(\omega)$ with (solid line) and without (dashed line) vertex corrections.

magnetic Brillouin zone. These optical transitions set in near 2Δ and form a broad and extended continuum due to transitions also far away from the Fermi lines.

In the optical region VC increase $\sigma(\omega)$ slightly at frequencies not too far away from 2Δ . This increase agrees with Eq.(67) because the second term on the right-hand side is due to VC and it is positive because the elements of \hat{X}_2 are small compared to unity. The influence of VC at small frequencies is illustrated in greater detail in Fig.4. First, VC increase the static value $\sigma(0)$ substantially. One reason for this is that the continuity equation for the charge density yields in the presence of a momentum-dependent order parameter an additional contribution to the current, given by the second term in Eq.(2). However, $\sigma(0)$ is not only below but also above T_c enhanced by VC. This increase is due to the renormalization of

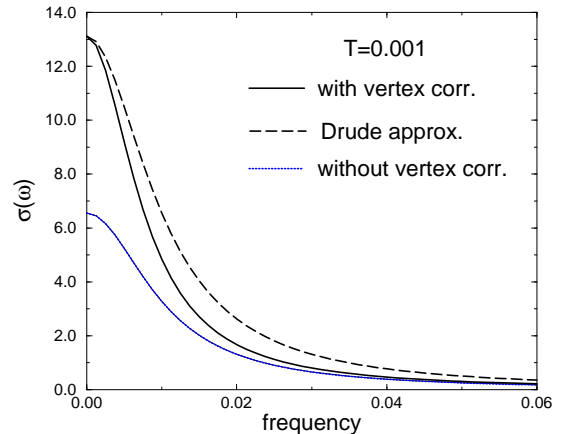


FIG. 4: Low-frequency behavior of $\sigma(\omega)$ with (solid curve) and without (dotted curve) vertex corrections. The dashed curve is a Lorentzian with the same value $\sigma(0)$ as the solid curve.

the one-particle energies. The resulting increase of $\sigma(0)$ has in our approach to be ascribed to VC because only a non-trivial vertex allows to fulfill the continuity equation, see Eq.(18). Secondly, the dashed curve in Fig.4, representing a Lorentzian with the same $\sigma(0)$ as for the solid line, illustrates the narrowing of the Drude peak with increasing frequency. This effect is induced by the frequency dependence of the vertex. The figure shows that the solid line approaches at larger frequencies the curve without VC (dotted line) which is a Lorentzian. This crossover takes place at the impurity scattering rate $1/\tau$. Fig.4 also shows that the effect of VC cannot be simulated in a theory without VC by a suitable redefinition of the current. The use of the bare current (first term in Eq.(2)) would result in a violation of the continuity equation and miss the enhancement of $\sigma(\omega)$ at low frequencies. On the other hand, the use of a current derived from the continuity equation as in Eq.(2) would yield the dashed curve in Fig.4 and would thus overestimate $\sigma(\omega)$ at large frequencies.

Fig.5 shows the temperature dependence of the restricted optical sum W and its low-frequency part, the Drude weight W_D . VC affect W in a two-fold way: They enhance the weak temperature dependence of W , calculated without VC (dot-dashed line), and also increase substantially the absolute value of W . The optical spectral weight $W - W_D$ is expected to set in below T_c in a square-root manner and to be rather independent of VC. Thus the enhancement of W and its stronger temperature dependence by VC should be related to the low-frequency part of $\sigma(\omega)$, i.e., to W_D , which is in agreement with the dashed and dotted curves in Fig.5.

Decreasing t' means that the length of the remnant Fermi lines becomes smaller until they shrink to points along the diagonals for $t' = 0$ as in a d-wave superconduc-

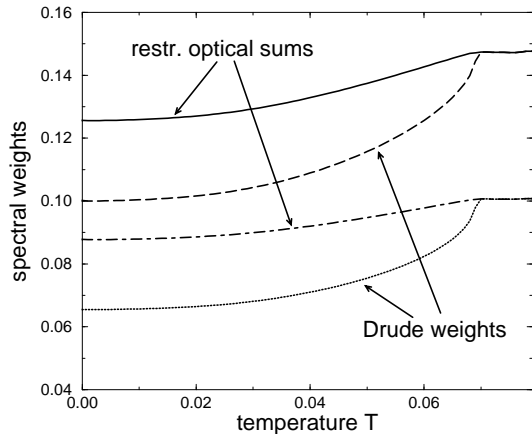


FIG. 5: Restricted optical sums with (solid line) and without (dot-dashed line) vertex corrections, and Drude weights with (dashed line) and without (dotted line) vertex corrections.

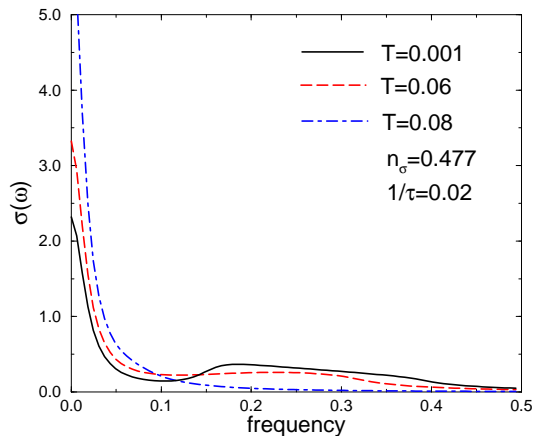


FIG. 6: Optical conductivity $\sigma(\omega)$ for $T = 0$, $\Delta = 0.197$ (solid line), $T = 0.06$, $\Delta = 0.158$ (dashed line), and $T = 0.08$, $\Delta = 0.041$ (dot-dashed line).

tor. Thus the ratio W_D/W should decrease with t' . The solid line in Fig.6, calculated with $t' = 0.05$, $T = 0$, $n_\sigma = 0.48$, $1/\tau = 0.03$, illustrates that this indeed is the case. Most of the spectral weight resides now in a very broad and extended high-frequency structure above $2\Delta \sim 0.35$,

only a small part of W is left for the Drude peak. With increasing temperature the length of the Fermi lines increases and the spectral weight is shifted from the optical region to the Drude peak, as shown by the dashed and dot-dashed lines in this figure.

In conclusion, we have calculated the optical conductivity $\sigma(\omega)$ of a two-dimensional d-CDW conductor taking into account vertex corrections. The employed formulation can easily be generalized to an arbitrary symmetry of the CDW state and to a general band structure. We have addressed and solved the problem of a proper definition of the current to be used in calculating $\sigma(\omega)$. Defining the current via the continuity equation both the renormalization of the one-particle energies due to the interaction causing the CDW as well as an additional term due to the momentum dependence of the CDW order parameter enter. Using this renormalized current and bare vertices yields a $\sigma(\omega)$ which is shown to be correct only in the limit $\omega \rightarrow 0$. On the other hand, using bare vertices and the bare electron dispersion violates in general the continuity equation for the charge density and gives a $\sigma(\omega)$ which is correct only at large frequencies. The proposed solution is to use bare current vertices but to include vertex and the corresponding self-energy corrections. In this way the continuity equation is explicitly fulfilled and the frequency dependence of the vertex interpolates smoothly from the strongly renormalized regime at low to the unrenormalized regime at high frequencies. This behavior is also visible in the numerically calculated conductivity curves. These calculations show the spectral features of the Drude-like peak at low and the transitions across the gap at high frequencies and their dependence on temperature and the next-nearest neighbor hopping constant t' . Remarkable is also that the temperature dependence of the restricted optical sum W (i.e., the spectral weight integrated over all frequencies) between $T = 0$ and $T = T_c$ is enhanced by vertex corrections. This may be interpreted as a violation of the sum rule by about 10 per cents in that interval. This as well as the other above predictions may help to identify experimentally unconventional CDW's.

Acknowledgments

The authors would like to thank I.V. Gornyi, A. Greco, C. Honerkamp, and M.N. Kiselev for valuable discussions.

* On leave from Petersburg Nuclear Physics Institute, Gatchina 188300, Russia.

¹ T.C. Hsu, J.B. Marston, and I. Affleck, Phys. Rev. B **43**, 2866 (1991)

² K. Maki, B. Dóra and A. Virosztek, AIP Conference Proceedings **695**, 10 (2003), and references therein

³ K. Maki, B. Dóra, M. Kartsovnik, A. Virosztek, B. Korin-Hamzić, and M. Basletić, Phys. Rev. Lett. B **90**, 256402 (2003)

⁴ A.H. Castro Neto, Phys. Rev. Lett. **86**, 4382 (2001)

⁵ I. Affleck and J.B. Marston, Phys. Rev. B **37**, 3774 (1988)

⁶ E. Cappelluti and R. Zeyher, Phys. Rev. B **59**, 6475 (1999)

- ⁷ L. Benfatto, S. Caprara, C. Di Castro, Eur. Phys. J.B. **17**, 95 (2000)
- ⁸ S. Chakravarty, C. Nayak, and S. Tewari, Phys. Rev. B **63**, 100504 (2003)
- ⁹ A. Iyengar, J. Stajic, Y.-J. Kao and K. Levin, Phys. Rev. Lett. **90**, 187003 (2003)
- ¹⁰ V. Oganesyan and I. Ussishkin, Phys. Rev. B **70**, 054503 (2004)
- ¹¹ D.N. Aristov and R. Zeyher, cond-mat/0405194
- ¹² B. Valenzuela, E.J. Nicol, and J.P. Carbotte, cond-mat/0407497
- ¹³ E. Cappelluti and R. Zeyher, Europh. Lett. **49**, 487 (2000)
- ¹⁴ R. Zeyher and E. Cappelluti, Physica C**341-348**, 121 (2000)
- ¹⁵ S. Chakravarty, H-Y Kee, and Ch. Nayak, Int. J. Mod. Phys. B **15**, 2901 (2001)
- ¹⁶ S. Chakravarty, Ch. Nayak, S. Tewari, and X. Yang, Phys. Rev. Lett. **89**, 277003 (2002)
- ¹⁷ S. Chakravarty, Ch. Nayak, and S. Tewari, Phys. Rev. B **68**, 100504 (2003)
- ¹⁸ A. Greco and R. Zeyher, Phys. Rev. B **70**, 024518 (2004)
- ¹⁹ D.N. Aristov and R. Zeyher, Phys. Rev. B **70**, 212511 (2004)
- ²⁰ G. Baym and L.P. Kadanoff, Phys. Rev. **124**, 287 (1961)
- ²¹ L. Benfatto, S.G. Sharapov, N. Andrenacci, and H. Beck, Phys. Rev. B **71**, 104511 (2005)
- ²² J.S. Langer, Phys. Rev. **127**, 5 (1962).